Stem Cell Reports
Article

ISSCR

OPEN ACCESS

Primary Ciliary Deficits in the Dentate Gyrus of Fragile X Syndrome

Bumwhee Lee,[1] Shree Panda,[1] and Hye Young Lee[1,*]
[1]The Department of Cellular and Integrative Physiology, the University of Texas Health Science Center at San Antonio, San Antonio, TX, USA
*Correspondence: leeh6@uthscsa.edu
https://doi.org/10.1016/j.stemcr.2020.07.001

SUMMARY

The primary cilium is the non-motile cilium present in most mammalian cell types and functions as an antenna for cells to sense signals. Ablating primary cilia in postnatal newborn neurons of the dentate gyrus (DG) results in both reduced dendritic arborization and synaptic strength, leading to hippocampal-dependent learning and memory deficits. Fragile X syndrome (FXS) is a common form of inheritance for intellectual disabilities with a high risk for autism spectrum disorders, and *Fmr1* KO mice, a mouse model for FXS, demonstrate deficits in newborn neuron differentiation, dendritic morphology, and memory formation in the DG. Here, we found that the number of primary cilia in *Fmr1* KO mice is reduced, specifically in the DG of the hippocampus. Moreover, this cilia loss was observed postnatally mainly in newborn neurons generated from the DG, implicating that these primary ciliary deficits may possibly contribute to the pathophysiology of FXS.

INTRODUCTION

More and more research suggests that neurons may sense and respond to their environment via a specialized organelle called a primary cilium (Green and Mykytyn, 2010), which grows from basal bodies and extends from the cell surface. The primary cilium is present in multiple cell types, including neurons in the brain, coordinates a series of signal transduction pathways, such as the sonic hedgehog (Shh), Wnt, and platelet-derived growth factor receptor α pathways, and relays information from the extracellular environment into the cell (Veland et al., 2009). Defective formation or function of primary cilia is implicated in the pathogenesis of many human developmental disorders and diseases, collectively termed ciliopathies (Badano et al., 2006; Green and Mykytyn, 2010). Ciliopathy patients display a range of neurological disorders (Lee and Gleeson, 2010), including cognitive deficits and behavioral phenotypes, thereby highlighting the importance of primary cilia function within the brain. While defective primary cilia leading to disruption of Shh signaling results in impaired survival and patterning of the embryonic mouse brain during development (Huangfu et al., 2003), after birth, primary cilia are required for proper proliferation and differentiation of granule neuron precursors (GNPs) in multiple brain regions, including in the dentate gyrus (DG) (Breunig et al., 2008; Han et al., 2008). Proper proliferation of GNPs in the DG requires primary cilia to respond to Shh signaling for postnatal hippocampal development (Breunig et al., 2008; Han et al., 2008). Primary cilia are also known to be critical players for neuronal maturation in the DG; conditional deletion of the primary cilia in adult-born neurons showed severe defects in dendritic arborization and synapse formation (Kumamoto et al., 2012), and conditionally ablated primary cilia in adult stem cells in the DG showed decreased newborn neuron production, which resulted in defects in hippocampal-dependent learning and memory (Amador-Arjona et al., 2011), which often are phenotypes of neurodevelopmental disorders. Although growing evidence indicates that primary cilia are implicated in brain development and intellectual disabilities, the functional role of primary cilia in neurodevelopmental disorders, such as fragile X syndrome (FXS) is largely unknown.

FXS is the most common monogenic cause of autism spectrum disorder, and is driven by the silencing of the fragile X mental retardation 1 (*FMR1*) gene leading to a range of developmental deficits, including intellectual disabilities and cognitive impairment. The *FMR1* gene encodes for the fragile X mental retardation protein (FMRP), which is an mRNA-binding protein and is expressed in the cell body, dendrites, and postsynaptic spines of neurons (Antar et al., 2004; Lee et al., 2011). The mouse model of FXS, the *Fmr1* knockout (KO) mouse, displays phenotypes similar to symptoms in the human condition, including cognitive deficits, hyperactivity, increased repetitive behaviors, and social deficits (Lee et al., 2018; Spencer et al., 2011). *Fmr1* KO mice are known to lose synaptic strength and to have hippocampal-dependent learning and memory deficits (Guo et al., 2011), which are phenotypes that are also shown by primary cilia loss in the DG (Rhee et al., 2016; Amador-Arjona et al., 2011). Furthermore, previous reports also revealed that *Fmr1* KO mice show reduced neuronal differentiation and dendritic complexity in postnatal newborn neurons in the DG (Guo et al., 2011; Luo et al., 2010), which are other phenotypes that are also shown in ciliary deficits (Amador-Arjona et al.,

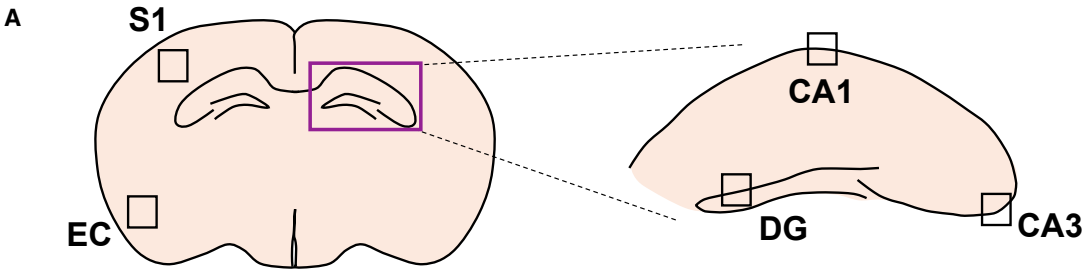

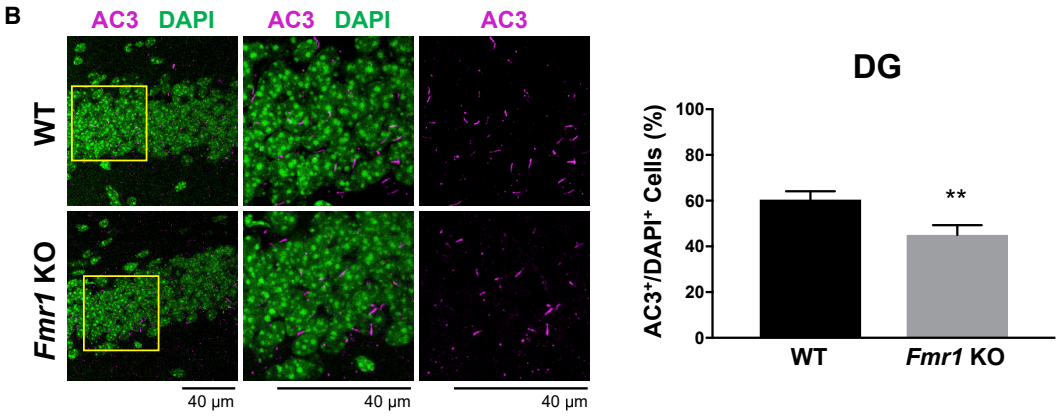

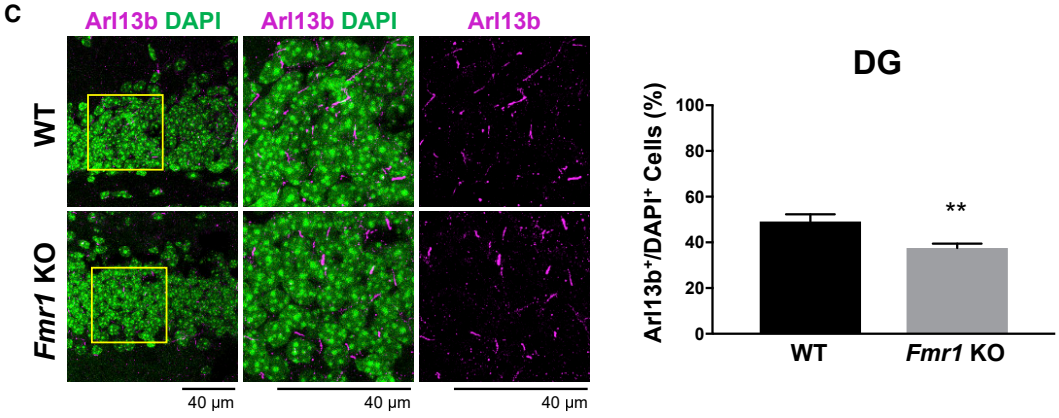

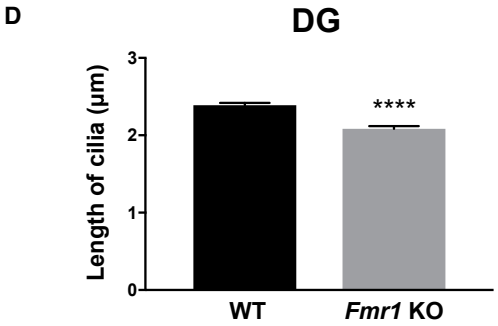

(legend on next page)

2011; Kumamoto et al., 2012). Given these shared phenotypes between losing FMRP and losing primary cilia in the DG, investigating whether primary cilia contribute to the pathophysiology of FXS can be important in understanding this disorder.

Our study is aimed at finding a link between primary cilia and neurodevelopmental disorders using a mouse model of FXS. Here, we demonstrate that the number of primary cilia was significantly reduced in the DG, but not altered in the somatosensory cortex, entorhinal cortex, and hippocampus proper (CA1 and CA3) in *Fmr1* KO mice compared with wild-type (WT) mice. When we further investigated primary cilia in various prenatal and postnatal developmental stages, we found a significant reduction in the number of primary cilia in the DG of *Fmr1* KO mice after postnatal day 14 (P14), but not in earlier postnatal ages or in embryos. Furthermore, the primary cilia loss in the DG of *Fmr1* KO mice was specifically found in mature granule neurons, especially in newborn neurons differentiated from the subgranular zone (SGZ) in the DG. Taken altogether, these results show primary cilia deficits in the DG of *Fmr1* KO mice, implicating that these deficits may possibly contribute to the pathophysiology of FXS.

RESULTS

Primary Cilia Are Significantly Reduced in the DG of Adult *Fmr1* KO Mice

To investigate primary cilia in *Fmr1* KO mice, we analyzed primary cilia in the hippocampus and the cortical area, where *Fmr1* KO mice show neuronal deficits associated with cognitive behavioral phenotypes in FXS (Bureau et al., 2008; Eadie et al., 2012), and where primary cilia are known to mediate cognitive function (Berbari et al., 2014). We examined primary cilia in the Ammon's horn (CA1 and CA3) and the DG of the hippocampus, and the somatosensory (S1) and entorhinal cortex (EC) of the cortical area (Figure 1A). Brain sections from adult WT or *Fmr1* KO mice were immunostained for type 3 adenylyl cyclase (AC3), a marker for primary cilia, and nuclear stained with 4′,6-diamidino-2-phenylindole (DAPI), then the percentage of $AC3^+$ cells were counted by normalizing with the total number of cells ($DAPI^+$ cells). As a result, among the brain regions that we investigated, the DG of *Fmr1* KO mice specifically showed a significant reduction (15.96% lower) in the number of primary cilia ($AC3^+$/$DAPI^+$ cells) compared with WT mice (Figure 1B). Notably, the number of primary cilia determined by another primary cilia marker, adenosine diphosphate (ADP)-ribosylation factor-like protein 13b (Arl13b), was still significantly decreased in *Fmr1* KO mice compared with WT mice (Figure 1C), implicating that the reduction of $AC3^+$ cells was not due to the reduction in AC3 expression levels, but due to the primary cilia loss. Given that ciliopathies often also demonstrate shorter primary cilia (Hernandez-Hernandez et al., 2013; Tuz et al., 2014), we investigated primary cilia length, which showed that *Fmr1* KO mice have shorter primary cilia compared with WT mice in the DG (Figure 1D). Since basal bodies template primary cilia formation and can mediate primary cilia deficits, we further checked if the DG of *Fmr1* KO mice show basal body deficits by immunostaining pericentrin, which identifies basal bodies of mouse photoreceptors (Mühlhans et al., 2011). As a result, Figure S1 shows that pericentrin adjacently localizes with $AC3^+$ primary cilia (marked with white arrows), and no significant reduction in number was observed in *Fmr1* KO mice compared with WT mice, indicating that the reduction of primary cilia in *Fmr1* KO mice is not mediated by basal body deficits. Finally, deficits in primary cilia are specific to the DG among the brain regions we investigated, as the number of primary cilia in the CA1, CA3, S1, and EC showed no significant difference between WT and *Fmr1* KO mice as shown in Figure 2. Taken together, our results demonstrate deficits in the number and the length of primary cilia in the DG of *Fmr1* KO mice.

Fmr1 KO Mice Show Age-Dependent Primary Cilia Deficits

Given that the DG developmental period extends from prenatal to postnatal days (Yu et al., 2014), we investigated primary cilia expression in the DG of WT or *Fmr1* KO mice from the prenatal stage (embryonic day 18.5 [E18.5]) through the postnatal stages (P0, P7, P10, P14, P30, and P60) to determine when the primary cilia deficits occur (Figure 3). As a result, although primary cilia were present in both WT and *Fmr1* KO mice throughout the prenatal to postnatal ages in the DG, increased numbers of primary cilia were found in WT mice as the DG developed until P30, while primary cilia in *Fmr1* KO mice remained at a consistently significant lower number at P14, P30, and P60 compared with WT mice

Figure 1. The Number and the Length of Primary Cilia Are Reduced in the DG of *Fmr1* KO Mice

(A) Schematic view of the hippocampus (CA1, CA3, and DG), and the cortex (S1 and EC), where primary cilia were investigated.

(B and C) Left: immunostaining of (B) AC3 (magenta) or (C) Arl13b (magenta) with DAPI nuclear staining (green) in the DG of P60 WT or *Fmr1* KO mice. Higher magnifications of the left images (yellow boxes) are shown in the middle and right panels. Right: quantification of the percentage of (B) $AC3^+$ or (C) $Arl13b^+$ cells among $DAPI^+$ cells in the DG.

(D) Quantification of the length of $AC3^+$ primary cilia in the DG of P60 WT or *Fmr1* KO mice.

n = 8, mean ± SEM, Student's unpaired t test. $^{**}p < 0.01$, $^{****}p < 0.0001$. See also Figure S1.

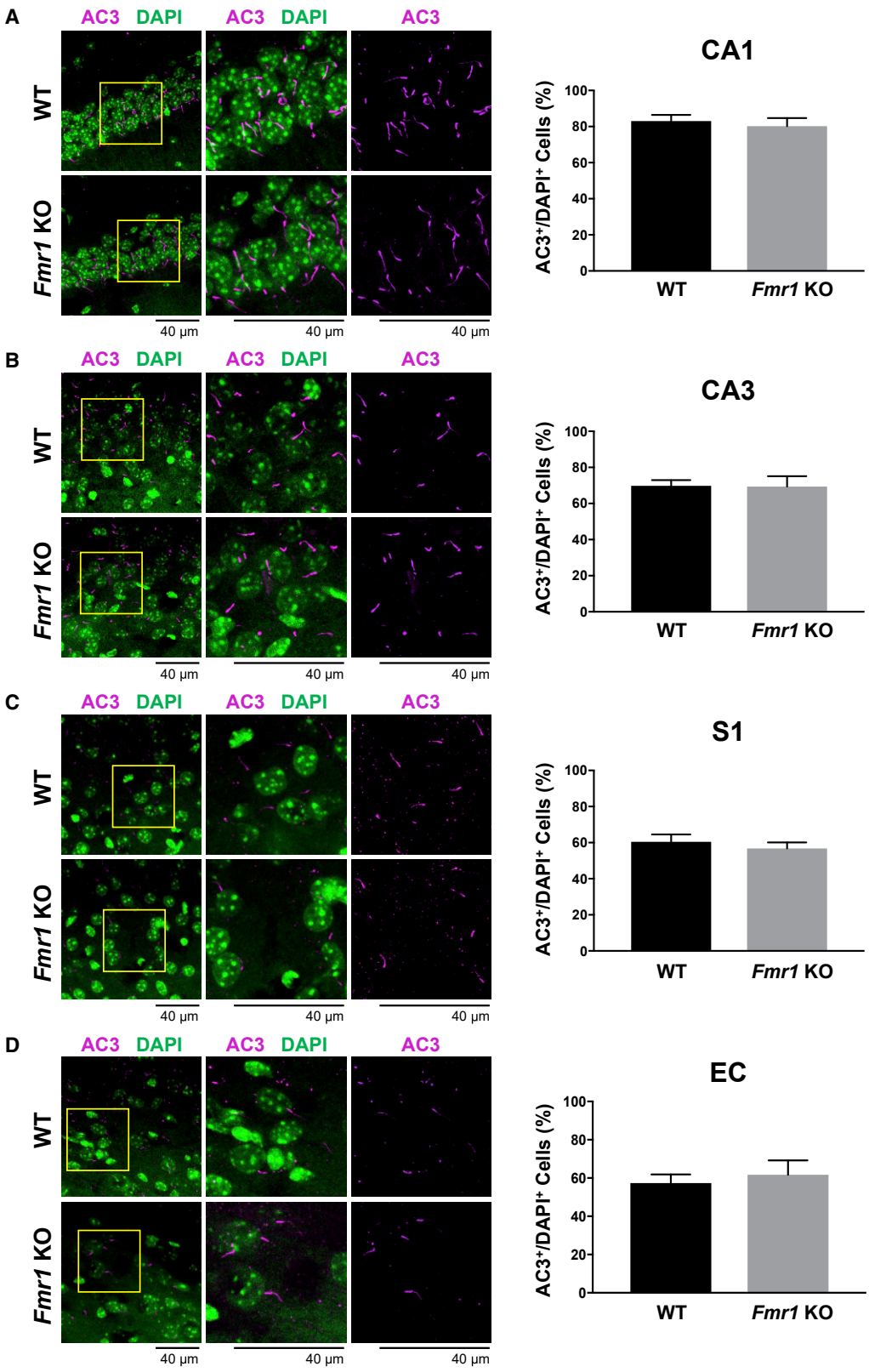

(legend on next page)

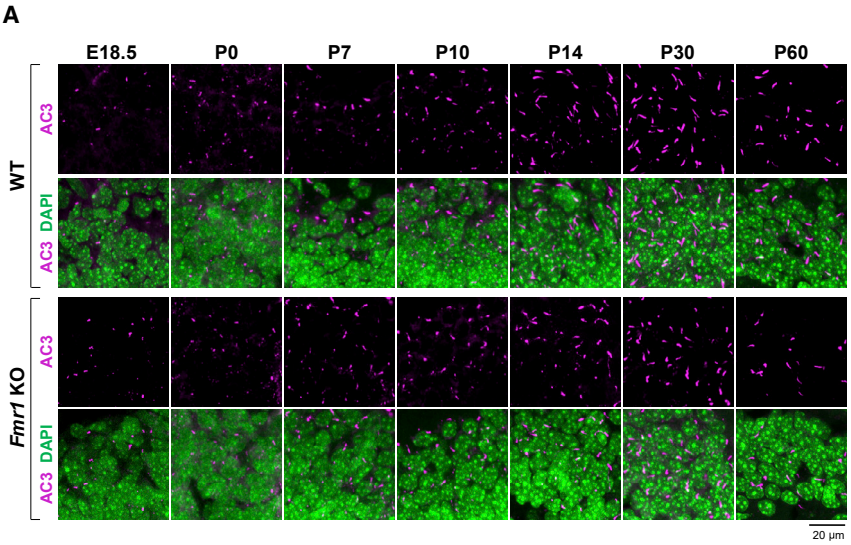

Figure 3. Primary Cilia Loss in the DG of *Fmr1* KO Mice Is Age Dependent

Brain sections were prepared from WT or *Fmr1* KO mice at E18.5, P0, P7, P10, P14, P30, and P60.

(A) Immunostaining of AC3 (magenta) with DAPI nuclear staining (green) in the DG of WT or *Fmr1* KO mice. $AC3^+$ primary cilia are shown in upper panels of WT and *Fmr1* KO mice, and $AC3^+$ primary cilia with $DAPI^+$ cells are shown in lower panels of WT and *Fmr1* KO mice.

(B) Quantification of the percentage of $AC3^+$ cells among $DAPI^+$ cells in the DG of WT and *Fmr1* KO mice at E18.5, P0, P7, P10, P14, P30, and P60.

n = 8, mean ± SEM, Student's unpaired t test. *p < 0.05, **p < 0.01, ****p < 0.0001.

(Figure 3); the percentage of ciliated cells in *Fmr1* KO mice was 14.70% lower at P14, 21.44% lower at P30, and 7.95% lower at P60 compared with WT mice (Figure 3B). Although we focused on the significant and consistent reduction of the number of primary cilia from P14 to P60, notably, the number of primary cilia showed a transient increase at P7 in *Fmr1* KO mice. Taken together, we demonstrate that a decreased number of primary cilia was observed from the age of P14 in the DG of *Fmr1* KO mice, which implicates that the primary ciliary loss is age dependent.

Primary Cilia Deficits Are Shown in Mature Granule Neurons of the DG in *Fmr1* KO Mice

As the DG forms around the first week of postnatal development, the neural progenitor cells (NPCs) settle at the border between the granule cell layer (GCL) and the hilus in the SGZ, where cells differentiate into granule neurons as they migrate into the GCL and project axons into the molecular layer (Li and Pleasure, 2005). This process persists throughout their lifetime in the GCL. Therefore, we next examined whether primary cilia deficits are specific to the differentiation status or to the type of cells in DG by determining the number of primary cilia in mature granule neurons ($NeuN^+$ or $calbindin^+$), NPCs ($BLBP^+$), or astrocytes ($S100\beta^+$) in the DG of WT or *Fmr1* KO mice. As a result, the number of primary cilia was significantly reduced in $NeuN^+$ or $calbindin^+$ mature granule neurons in the DG of *Fmr1* KO mice at P14, P30, and P60, but not in earlier ages (Figures 4A, 4B, and S2). However, in $NeuN^-$ cells, where a lower density of primary cilia was observed

Figure 2. Primary Cilia Deficits Are Not Observed in the CA1 and CA3 Regions of the Hippocampus, and S1 and EC of the Cortex in *Fmr1* KO Mice

(A–D) Left: immunostaining of AC3 (magenta) with DAPI nuclear staining (green) in the brains of P60 WT or *Fmr1* KO mice. The (A) hippocampal CA1 (CA1), (B) hippocampal CA3 (CA3), (C) somatosensory cortex (S1), and (D) entorhinal cortex (EC) were imaged and higher magnifications of the left images (yellow boxes) are shown in the middle and right panels. Right: quantification of the percentage of $AC3^+$ cells among $DAPI^+$ cells in the indicated brain region.

n = 8, mean ± SEM. Student's unpaired t test.

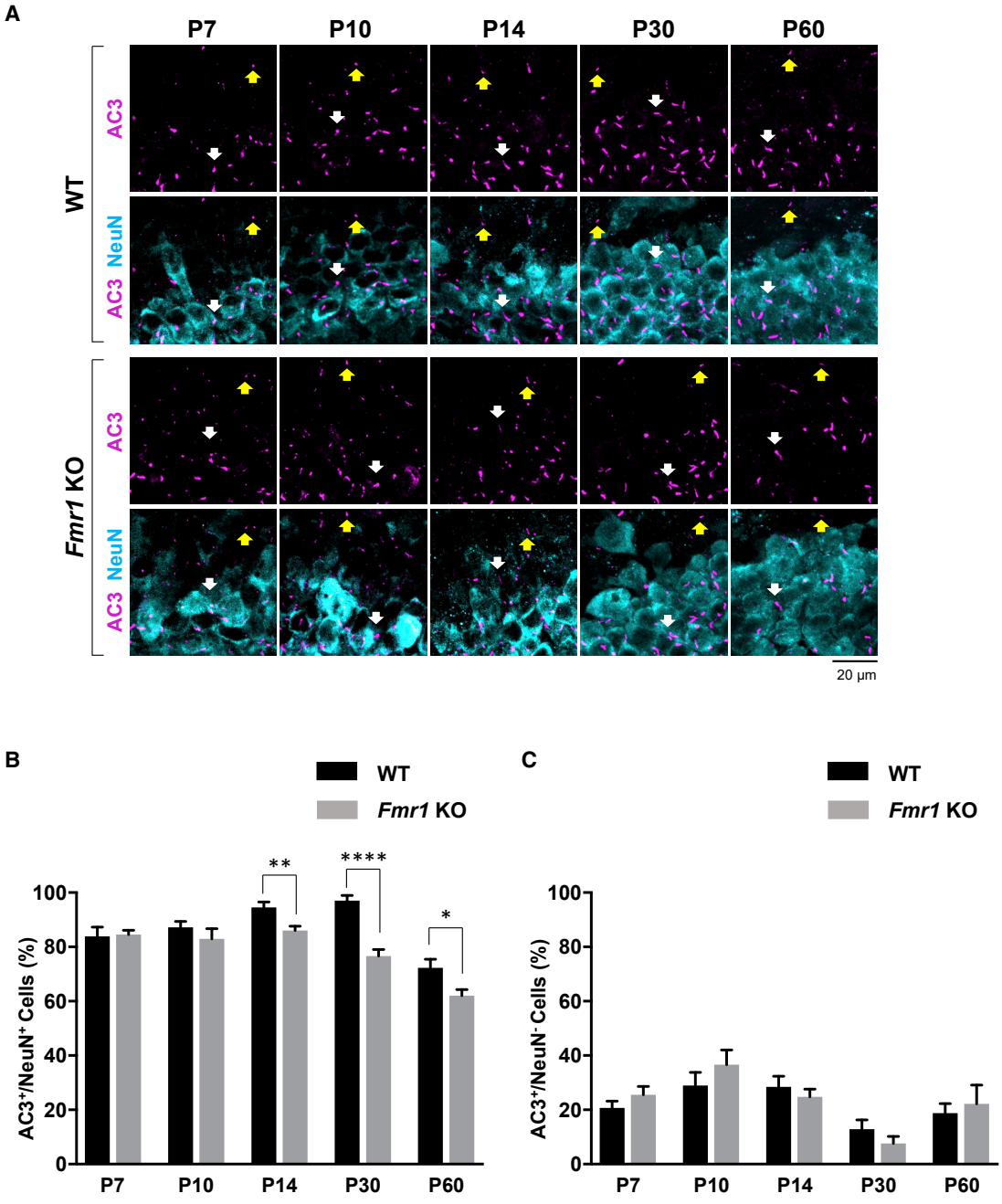

Figure 4. Age-Dependent Primary Cilia Deficits Are Found Specifically in NeuN$^+$ Mature Granule Neurons of *Fmr1* KO Mice

(A) Immunostaining of AC3 (magenta) and NeuN (cyan) in the DG of P7, P10, P14, P30, and P60 WT or *Fmr1* KO mice. AC3$^+$ primary cilia are shown in upper panels of WT and *Fmr1* KO mice, and AC3$^+$ primary cilia with NeuN$^+$ cells are shown in lower panels of WT and *Fmr1* KO mice. White arrows, AC3$^+$;NeuN$^+$ cells; yellow arrows, AC3$^+$;NeuN$^-$ cells.

(B and C) Quantification of the percentage of AC3$^+$ cells among (B) NeuN$^+$ cells or (C) NeuN$^-$ cells. n = 8, mean ± SEM. Student's unpaired t test. *p < 0.05, **p < 0.01, ****p < 0.0001. See also Figures S2 and S3.

compared with NeuN$^+$ cells, no significant difference in primary cilia number was observed at any ages tested (P7, P10, P14, P30, and P60) in the DG of *Fmr1* KO mice (Figures 4A and 4C). Notably, upon investigating primary cilia in NPCs (BLBP$^+$), no reduction in primary cilia number was observed in the DG of P30 or P60 *Fmr1* KO mice compared with WT mice (Figures 5A and 5B), implicating that the primary cilia deficits observed in *Fmr1* KO mice are specific to

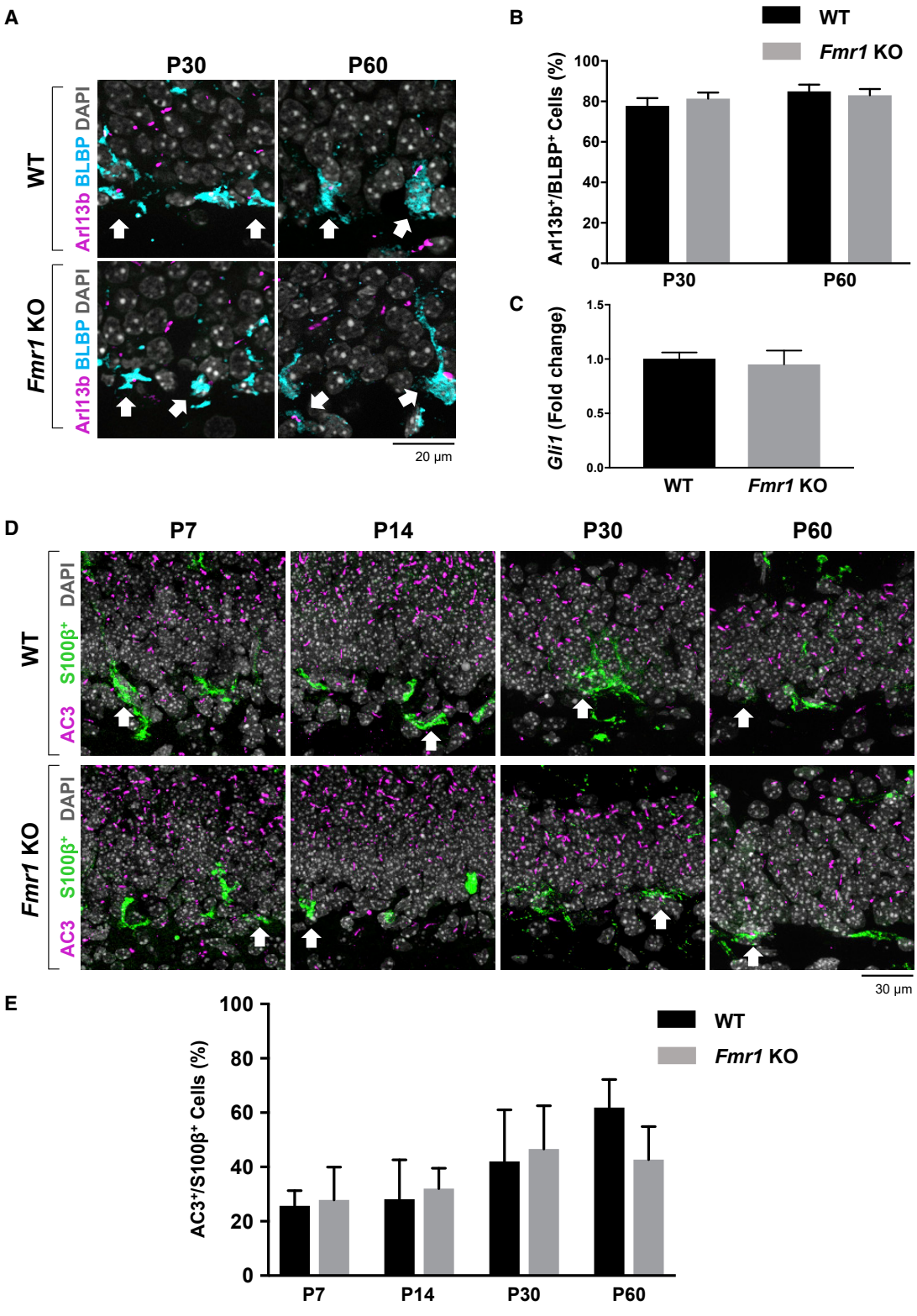

(legend on next page)

the differentiation status of cells in DG (mature granule neurons). Since primary cilia are well known to mediate Shh signaling, we further determined whether primary cilia loss in the DG of *Fmr1* KO mice contributes to Shh signaling by measuring *Gli1* mRNA expression, an indicator of Shh signaling, using qRT-PCR. Figure 5C demonstrates that there is no significant change in *Gli1* mRNA levels in the DG of *Fmr1* KO mice, indicating no significant change in Shh signaling. Since Gli1 is known to be mainly detected at high levels in the inner area of the DG, and mediates Shh signaling mainly in NPCs of the DG (Han et al., 2008), our result of no significant change in *Gli1* mRNA levels supports the observation of no significant reduction of primary cilia number in NPCs in the DG of *Fmr1* KO mice. Finally, astrocytes (S100β$^+$) in the DG of *Fmr1* KO mice showed no significant reduction of primary cilia number (Figures 5D and 5E), implicating that the primary cilia deficits observed in *Fmr1* KO mice are specific to the type of cells in DG (granule neurons).

Given that neurogenesis in the DG was previously shown to be reduced in *Fmr1* KO mice (Luo et al., 2010), next we checked the neuronal populations in the DG of WT or *Fmr1* KO mice at various ages to know if the primary cilia density was affected by the neuronal density (Figure S3). Although the proportion of mature granule neurons (NeuN$^+$) to total number of cells (DAPI$^+$) in the DG of *Fmr1* KO mice was increased at P7 and P10 compared with WT mice, there were no significant differences at P14, P30, and P60 (Figure S3B), the ages which showed the decreased primary cilia expression in mature granule neurons (Figures 4A, 4B, and S2), implicating that the primary cilia deficits are not affected by the neuronal density in the DG of *Fmr1* KO mice. Taken altogether, our results demonstrate that the reduction of primary cilia in the DG of *Fmr1* KO mice is specifically found in mature granule neurons and is age dependent.

Primary Cilia Deficits Are Observed in Newborn Neurons from SGZ, but Not in Neurons from DNe

The DG is one of the two areas of the brain where neurogenesis occurs postnatally (Eriksson et al., 1998). In the prenatal stage and the early postnatal stage, postmitotic neurons and GNPs migrate to the DG from the dentate neuroepithelium (DNe) (Altman and Bayer, 1990). The GNPs are then transformed into neural stem cells in the SGZ of the DG and begin producing dentate granule cells, which result in the majority of newborn granule cells in the GCL (Li and Pleasure, 2005). Therefore, the granule neuronal population in the DG is heterogeneous; they originate from either the DNe or the SGZ (Urbán and Guillemot, 2014). Meanwhile, most primary cilia assemble between 14 and 21 days after the birth of the newborn granule cells in the GCL of the DG (Kumamoto et al., 2012). Given that primary cilia loss in neurons of the DG was shown from around P14 in *Fmr1* KO mice, and that neuronal maturation takes 14–21 days, we hypothesized that the primary cilia loss in the DG of *Fmr1* KO mice was triggered in newborn neurons from the SGZ, and that these could account for the cilia loss in P14. To investigate primary ciliogenesis in newborn neurons from the DNe or the SGZ, we performed an intraperitoneal injection of 5-bromo-2′-deoxyuridine (BrdU) in various developmental stages. Given the development of DG begins around E13.5 (Yu et al., 2014), we injected BrdU at E12.5 (single injection) to track DNe-newborn neurons, and at E15.5 (single injection), P7–8, P30–31, or P60–61 (three times daily for 2 days, 8 h apart) to track SGZ-newborn neurons (Figure 6). After 28 days from the last BrdU injection for the neuronal maturation (at P21, P24, P36, P59, or P89, respectively), we investigated the primary cilia in newborn neurons originating at the ages of E12.5, E15.5, P7–8, P30–31, or P60–61 of WT or *Fmr1* KO mice (Figures 6A and 6B). As a result, newborn neurons from embryonic development were positioned in the outer layer of the GCL (BrdU injection at E12.5 or E15.5 in Figure 6A), while postnatal newborn neurons migrated into the inner and middle layers of the GCL (BrdU injection at P7–8, P30–31, or P60–61 in Figure 6A) as indicated in a previous study (Mathews et al., 2010). We then analyzed the percentage of the primary cilia in newborn neurons (NeuN$^+$;BrdU$^+$) of WT or *Fmr1* KO mice (Figure 6C). As a result, while DNe-newborn neurons originating at E12.5 did not exhibit primary cilia loss in *Fmr1* KO mice, SGZ-newborn neurons originating at E15.5, P7–8, P30–31, or P60–61 showed

Figure 5. No Significant Change in the Number of Primary Cilia Is Found in NPCs (BLBP$^+$) or Astrocytes (S100β$^+$) in the DG of *Fmr1* KO Mice

(A) Immunostaining of Arl13b (magenta) and BLBP (cyan) with DAPI nuclear staining (gray) in the DG of P30 and P60 WT or *Fmr1* KO mice. White arrows, Arl13b$^+$;BLBP$^+$ cells.

(B) Quantification of the percentage of Arl13b$^+$ cells among BLBP$^+$ cells.

(C) *Gli1* mRNA level was analyzed by qRT-PCR in the DG of adult WT or *Fmr1* KO mice. Values of *Gli1* mRNA were normalized by housekeeping gene peptidylprolyl isomerase A (*Ppia*) mRNA levels.

(D) Immunostaining of AC3 (magenta) and S100β (green) with DAPI nuclear staining (gray) in the DG of P7, P14, P30, and P60 WT or *Fmr1* KO mice. White arrows, AC3$^+$;S100β$^+$ cells.

(E) Quantification of the percentage of AC3$^+$ cells among S100β$^+$ cells. n = 8 for immunostaining, n = 3 for qRT-PCR, mean ± SEM. Student's unpaired t test.

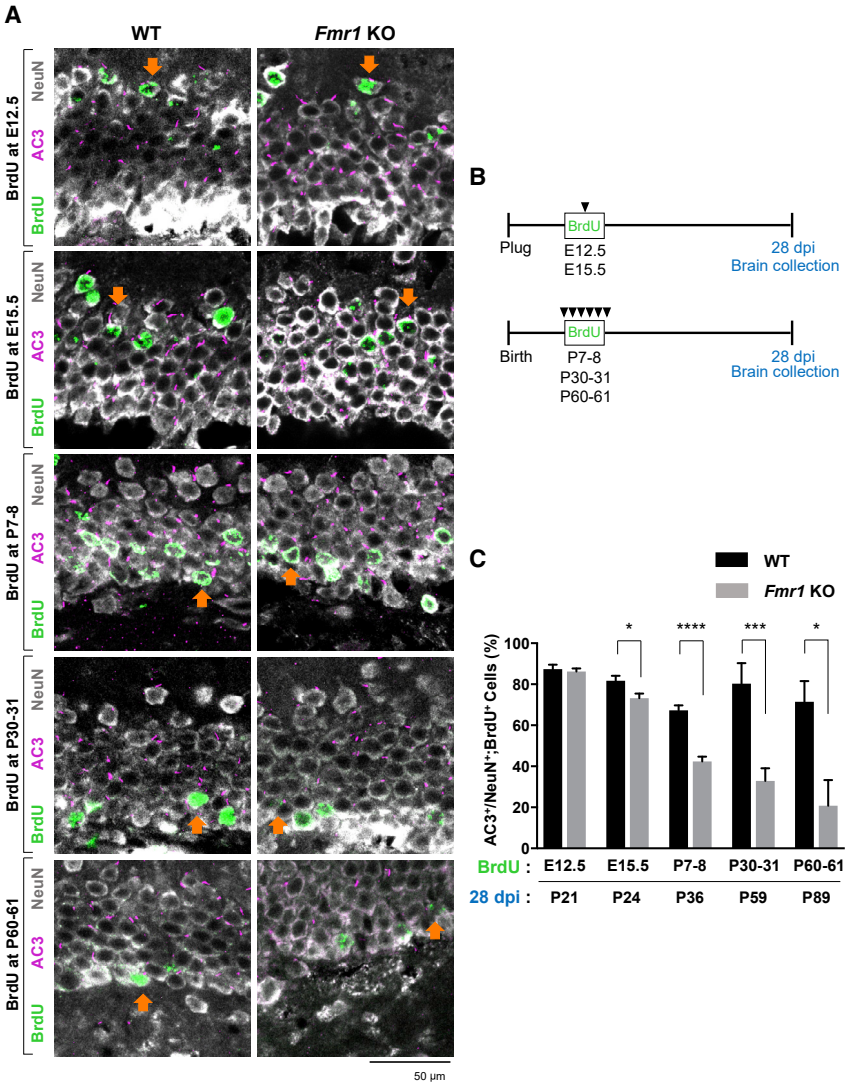

Figure 6. Newborn Neurons (NeuN$^+$;BrdU$^+$) Originated from the SGZ Exhibit Primary Cilia Loss in the DG of *Fmr1* KO Mice

BrdU was administrated by intraperitoneal injection into WT or *Fmr1* KO mice at E12.5, E15.5, P7–8, P30–31, or P60–61 followed by brain collection at 28 days post injection (dpi).

(A) Immunostaining of AC3 (magenta), NeuN (gray), and BrdU (green) in the DG of BrdU-treated WT or *Fmr1* KO mice. Orange arrows, AC3$^+$;NeuN$^+$;BrdU$^+$ cells. Inner layer (toward hilus) of the DG is located on the lower side of images.

(B) Schematic view of BrdU treatment and collection of WT or *Fmr1* KO mice.

(C) Quantification of the percentage of AC3$^+$ cells among NeuN$^+$;BrdU$^+$ newborn neurons originating at E12.5, E15.5, P7–8, P30–31, or P60–61 in WT and *Fmr1* KO mice (28 dpi: P21, P24, P36, P59, or P89).

n = 8–10, mean ± SEM, Student's unpaired t test. *p < 0.05, ***p < 0.001, ****p < 0.0001. See also Figures S4–S6.

significant reduction of primary cilia in the DG of *Fmr1* KO mice compared with WT mice (Figure 6C), indicating that there were primary cilia deficits in newborn neurons from the SGZ of the DG. A similar result was observed when using another neuronal marker, calbindin (Figure S4). Notably, total primary cilia number in NeuN$^+$ mature granule neurons from *Fmr1* KO mice at 28 days post-BrdU injection (at P21, P24, P36, P59, or P89, respectively) still show primary cilia deficits compared with WT mice as observed in Figures 4A, 4B, and S2, indicating that BrdU administration did not alter the primary cilia phenotype in *Fmr1* KO mice (data not shown).

Since previous studies revealed that *Fmr1* KO mice showed reduced neurogenesis but increased newly differentiated astrocytes in the DG (Guo et al., 2011; Luo et al., 2010), we also checked primary cilia in newly differentiated astrocytes (S100β$^+$;BrdU$^+$). As a result, the number of primary cilia in newly differentiated astrocytes did not show a significant difference between WT and *Fmr1* KO mice (Figure S5), implicating that primary cilia loss is specific to newborn neurons and is independent of the rate of differentiation to newborn neurons or newly differentiated astrocytes in the DG. Taken altogether, these results demonstrate that newborn neurons from the SGZ specifically show primary cilia deficits, indicating that the primary ciliary deficits are dependent on the origin of the cells in *Fmr1* KO mice.

DISCUSSION

Defective primary cilia have been associated with diverse human diseases, including Alström, Bardet-Biedl, Joubert,

Meckel-Gruber, and Oral-facial-digital type 1 syndromes (Badano et al., 2006). The pathology of these pleiotropic disorders includes intellectual disability and ataxia, suggesting that primary cilia are required for the proper development or function of the brain. In the DG, primary cilia are known to be required for proper proliferation and differentiation of the GNPs into granule neurons, which play crucial roles for learning and memory (Breunig et al., 2008; Han et al., 2008). Primary cilia are also known to be critical players for neuronal maturation in the DG (Amador-Arjona et al., 2011; Kumamoto et al., 2012). Although several recent works reported possible roles of primary cilia in neuronal development and brain behaviors, the contribution of primary cilia in normal brain function and brain disorders remains largely understudied; specifically, the role of primary cilia in neurodevelopmental disorders is largely unknown. In this study, we demonstrate that loss of FMRP leads to primary cilia deficits in a mouse model of FXS. In the DG of *Fmr1* KO mice, we found the reduction of primary cilia number and length, phenotypes observed in multiple ciliopathies, including Joubert and Bardet-Biedl syndromes (Hernandez-Hernandez et al., 2013; Tuz et al., 2014). Previous studies revealed the potential role of FMRP in newborn neurons, including decreases in dendritic length, complexity, and branch tip numbers observed in hippocampal newborn neurons from *Fmr1* KO mice (Guo et al., 2011), and the reductions in dendrite number, length, and branching in embryonic stem cells and induced pluripotent stem cells from human FXS patients (Castrén et al., 2005; Doers et al., 2014). Therefore, our results demonstrating primary cilia deficits in newborn granule neurons of the DG induced by FMRP loss, a condition of FXS, implicates the possible contribution of primary cilia to the pathophysiology of FXS given that primary cilia play a critical role for neuronal maturation of newborn neurons in the DG (Amador-Arjona et al., 2011; Kumamoto et al., 2012).

We demonstrated that the number of primary cilia is significantly reduced in the DG, but not in the CA1 or CA3 of the hippocampus or in the cortical areas (brain region specific) in adult *Fmr1* KO mice (Figures 1 and 2). We also showed that the loss of primary cilia is observed from ages around P14 and the deficit continues to adulthood (age dependent) in *Fmr1* KO mice (Figure 3). Therefore, our findings indicate that primary cilia loss in *Fmr1* KO mice occurs at a specific time and location. Moreover, we identified that the number of primary cilia shows a marked decrease in mature granule neurons in the DG of *Fmr1* KO mice from ages around P14, but primary cilia deficits were not found in NPCs (differentiation status specific) or astrocytes (cell type specific) in the DG of *Fmr1* KO mice (Figures 4, 5, and S2). The distinct origin of embryonic cells (DNe-origin) and NPCs (SGZ-origin) contributes to a heterogeneous mixture of the granule neuronal population in the DG (Urbán and Guillemot, 2014). Our BrdU-labeling experiments revealed that newborn neurons from the SGZ (SGZ-newborn neurons) lost primary cilia in *Fmr1* KO mice while newborn neurons from the DNe (DNe-newborn neurons) did not show primary cilia loss (origin specific) in *Fmr1* KO mice compared with WT mice (Figures 6 and S4). Moreover, the reduction of primary cilia number in SGZ-newborn neurons corresponds to the level of reduction shown in ciliopathies (Hernandez-Hernandez et al., 2013; Tuz et al., 2014). However, mechanisms underlying how newborn neurons from the SGZ specifically show primary cilia deficits in *Fmr1* KO mice need further investigations.

Our result demonstrates that the primary cilia loss in the absence of FMRP occurs between E12.5 and E15.5, and implicates that primary cilia deficits are mainly in the SGZ-newborn neurons rather than the DNe-newborn neurons (Figure 6). There may be a dramatic change in the conditions of cells during this critical period in the DG development between E12.5 and E15.5, which may cause the primary cilia deficits shown in mature granule neurons between P10 and P14 in the DG of *Fmr1* KO mice (Figure 4), given that both the primary cilia maturation and the neuronal differentiation take approximately 14–21 days (Kumamoto et al., 2012). One possible mechanism is that dramatic FMRP level changes, if detected in this critical period of primary cilia loss, can potentially contribute to primary cilia deficits detected in SGZ-newborn neurons from around P14 in *Fmr1* KO mice. However, when we checked whether there was any dramatic elevation in the expression levels of FMRP between E12.5 and E15.5, no significant difference in FMRP levels in the DNe or DG of WT embryos at E12.5, E15.5, and E18.5 was detected (Figure S6). This result demonstrates that FMRP levels may not be a critical factor in mediating the primary cilia loss transition in E12.5–E15.5 and P10–P14, but given that primary cilia loss is spatially and temporally controlled, and that FMRP is an mRNA-binding protein that associates with polyribosomes and regulates the trafficking, stability, and translation of mRNA (Laggerbauer et al., 2001; Lee et al., 2011), one potential scenario might be that FMRP contributes to the primary ciliogenesis directly or indirectly by regulating mRNAs which are critical for primary cilia formation or maintenance. The molecular mechanisms underlying primary cilia deficits in SGZ-newborn neurons of FXS can be further investigated by identifying FMRP mRNA targets and characterizing how FMRP regulates primary cilia. Our result also demonstrates ciliary loss specifically in the DG among the brain regions that we investigated (Figures 1 and 2), although FMRP, which expresses ubiquitously through the brain, does not show a specific higher expression in the DG compared with the CA1 and CA3 of the hippocampus (Zorio et al., 2017). Notably, the

DG is one of the two areas of the brain where neurogenesis occurs postnatally (Eriksson et al., 1998), therefore we believe that our findings can lead to exciting potential future studies as to whether another brain region, the olfactory bulb, where postnatal newborn neurons migrate to (Urbán and Guillemot, 2014), shows ciliogenesis deficits in *Fmr1* KO mice.

EXPERIMENTAL PROCEDURES

Animals

FVB.129P2-*Pde6b*$^{+}$ *Tyr*$^{c\text{-}ch}$/AntJ (control for *Fmr1* KO mice) and FVB.129P2-*Pde6b*$^{+}$ *Tyr*$^{c\text{-}ch}$ *Fmr1*^{tm1Cgr}/J (*Fmr1* KO mice) were purchased from Jackson Laboratory. Heterozygous females (*Fmr1*$^{+/-}$) were generated by crossing *Fmr1* KO female (*Fmr1*$^{-/-}$) and control male (*Fmr1*$^{+/y}$) mice, which were then crossed with control male (*Fmr1*$^{+/y}$) mice to obtain male *Fmr1* KO pups (*Fmr1*$^{-/y}$) and male WT control littermates (*Fmr1*$^{+/y}$). For BrdU injections, control mice and *Fmr1* KO mice were given intraperitoneal injections of BrdU. Mice for each genotype were chosen randomly for all experiments. All mice were housed in the university's animal facility which was maintained under normal humidity and temperature with 12 h periods of light and darkness. Food and water were provided *ad libitum*. The use and care of animals in this study followed the guidelines of the University of Texas Health Science Center at San Antonio (UTHSCSA) Institutional Animal Care and Use Committee (IACUC).

Embryo Collection

Embryos were collected through timed breeding of adult males and females with E0.5 being noon of the day the vaginal plug was detected. Plugged females were euthanized, and embryos were collected at E12.5, E15.5, and E18.5. Brains were dissected and fixed in 4% paraformaldehyde (PFA) (w/v) in 1× PBS for 2 h at 4°C, and then stored in 30% sucrose for 2 days. Embryonic brains were kept at −80°C after being embedded into embedding mold with Tissue-Plus O.C.T. Compound. Coronal sections (25 μm) were obtained by cryostat sectioning onto a Superfrost Plus slide. The sections were stored at −20°C until use for immunostaining.

Postnatal Brain Preparation

Postnatal mice at P7, P10, P14, P30, and P60 were anesthetized with isoflurane and perfused intracardially with PBS followed by 4% PFA, whereas P0 mice were decapitated without perfusion. Brains were dissected and fixed in 4% PFA in 1× PBS for 4 h at 4°C, and then stored in 30% sucrose for 2 days. Embryonic brains were kept at −80°C after being embedded into embedding mold with Tissue-Plus O.C.T. Compound. Coronal sections (25 μm) were obtained by cryostat sectioning onto a Superfrost Plus slide. The sections were stored at −20°C until used for immunostaining. For qRT-PCR, the DG was dissected as indicated previously (Hagihara et al., 2009) followed by RNA extraction.

BrdU Injections

To study the primary cilia in newborn neurons, BrdU was intraperitoneally injected into mice. For injection into mouse embryos, BrdU was injected once into pregnant females at E12.5 or E15.5 (15 mg kg^{-1} body weight at E12.5; 25 mg kg^{-1} body weight at E15.5), and perfused with 4% PFA 28 days after the injection. Postnatal mice (P7, P30, and P60) were injected with 50 mg kg^{-1} body weight of BrdU intraperitoneally three times, 8 h apart, for 2 days (six injections total) and perfused with 4% PFA 28 days after the last injection as described previously (Amador-Arjona et al., 2011).

Statistical Analysis

Significant differences were designated by Student's unpaired t test or one-way ANOVA. For all comparisons, values of $p < 0.05$ were considered statistically significant, and all data are presented as mean ± SEM. All the statistics showed that variances were similar between the groups that were being statistically compared. No statistical methods were used to pre-determine sample sizes, but all sample sizes are similar to those generally used in the field. Sample size (n) is indicated in each figure legend. None of the samples were excluded for the analysis.

Materials, Antibodies, Vaginal Plug Formation, RNA Extraction from Mouse Brains and qRT-PCR, Immunostaining, Imaging and Analysis, and Data Availability. See Supplemental Experimental Procedures for details.

SUPPLEMENTAL INFORMATION

Supplemental Information can be found online at https://doi.org/10.1016/j.stemcr.2020.07.001.

AUTHOR CONTRIBUTIONS

B.L. conceived the study, performed the experiments, including brain preparation, BrdU injection, immunostaining, analysis, and qRT-PCR, and wrote the manuscript. S.P. wrote the manuscript, performed the experiments, including immunostaining and analysis, and assisted with animal maintenance. H.Y.L. supervised the whole project and wrote the manuscript.

ACKNOWLEDGMENTS

We thank Manzoor A. Bhat and Bhat Lab members for technical support. This work was supported by UT System Rising STARs Award to H.Y.L.

Received: November 16, 2018
Revised: June 30, 2020
Accepted: July 1, 2020
Published: July 30, 2020

REFERENCES

Altman, J., and Bayer, S.A. (1990). Migration and distribution of two populations of hippocampal granule cell precursors during the perinatal and postnatal periods. J. Comp. Neurol. *301*, 365–381.

Amador-Arjona, A., Elliott, J., Miller, A., Ginbey, A., Pazour, G.J., Enikolopov, G., Roberts, A.J., and Terskikh, A.V. (2011). Primary cilia regulate proliferation of amplifying progenitors in adult hippocampus: implications for learning and memory. J. Neurosci. *31*, 9933–9944.

Antar, L.N., Afroz, R., Dictenberg, J.B., Carroll, R.C., and Bassell, G.J. (2004). Metabotropic glutamate receptor activation regulates fragile X mental retardation protein and FMR1 mRNA localization differentially in dendrites and at synapses. J. Neurosci. *24*, 2648–2655.

Badano, J.L., Mitsuma, N., Beales, P.L., and Katsanis, N. (2006). The ciliopathies: an emerging class of human genetic disorders. Annu. Rev. Genomics Hum. Genet. *7*, 125–148.

Berbari, N.F., Malarkey, E.B., Yazdi, S.M., McNair, A.D., Kippe, J.M., Croyle, M.J., Kraft, T.W., and Yoder, B.K. (2014). Hippocampal and cortical primary cilia are required for aversive memory in mice. PLoS One *9*, e106576.

Breunig, J.J., Sarkisian, M.R., Arellano, J.I., Morozov, Y.M., Ayoub, A.E., Sojitra, S., Wang, B., Flavell, R.A., Rakic, P., and Town, T. (2008). Primary cilia regulate hippocampal neurogenesis by mediating sonic hedgehog signaling. Proc. Natl. Acad. Sci. U S A *105*, 13127–13132.

Bureau, I., Shepherd, G.M., and Svoboda, K. (2008). Circuit and plasticity defects in the developing somatosensory cortex of FMR1 knock-out mice. J. Neurosci. *28*, 5178–5188.

Castrén, M., Tervonen, T., Kärkkäinen, V., Heinonen, S., Castrén, E., Larsson, K., Bakker, C.E., Oostra, B.A., and Akerman, K. (2005). Altered differentiation of neural stem cells in fragile X syndrome. Proc. Natl. Acad. Sci. U S A *102*, 17834–17839.

Doers, M.E., Musser, M.T., Nichol, R., Berndt, E.R., Baker, M., Gomez, T.M., Zhang, S.C., Abbeduto, L., and Bhattacharyya, A. (2014). iPSC-derived forebrain neurons from FXS individuals show defects in initial neurite outgrowth. Stem Cells Dev. *23*, 1777–1787.

Eadie, B.D., Cushman, J., Kannangara, T.S., Fanselow, M.S., and Christie, B.R. (2012). NMDA receptor hypofunction in the dentate gyrus and impaired context discrimination in adult Fmr1 knockout mice. Hippocampus *22*, 241–254.

Eriksson, P.S., Perfilieva, E., Björk-Eriksson, T., Alborn, A.M., Nordborg, C., Peterson, D.A., and Gage, F.H. (1998). Neurogenesis in the adult human hippocampus. Nat. Med. *4*, 1313–1317.

Green, J.A., and Mykytyn, K. (2010). Neuronal ciliary signaling in homeostasis and disease. Cell Mol. Life Sci. *67*, 3287–3297.

Guo, W., Allan, A.M., Zong, R., Zhang, L., Johnson, E.B., Schaller, E.G., Murthy, A.C., Goggin, S.L., Eisch, A.J., Oostra, B.A., et al. (2011). Ablation of Fmrp in adult neural stem cells disrupts hippocampus-dependent learning. Nat. Med. *17*, 559–565.

Hagihara, H., Toyama, K., Yamasaki, N., and Miyakawa, T. (2009). Dissection of hippocampal dentate gyrus from adult mouse. J. Vis. Exp., 1543.

Han, Y.G., Spassky, N., Romaguera-Ros, M., Garcia-Verdugo, J.M., Aguilar, A., Schneider-Maunoury, S., and Alvarez-Buylla, A. (2008). Hedgehog signaling and primary cilia are required for the formation of adult neural stem cells. Nat. Neurosci. *11*, 277–284.

Hernandez-Hernandez, V., Pravincumar, P., Diaz-Font, A., May-Simera, H., Jenkins, D., Knight, M., and Beales, P.L. (2013). Bardet-Biedl syndrome proteins control the cilia length through regulation of actin polymerization. Hum. Mol. Genet. *22*, 3858–3868.

Huangfu, D., Liu, A., Rakeman, A.S., Murcia, N.S., Niswander, L., and Anderson, K.V. (2003). Hedgehog signalling in the mouse requires intraflagellar transport proteins. Nature *426*, 83–87.

Kumamoto, N., Gu, Y., Wang, J., Janoschka, S., Takemaru, K., Levine, J., and Ge, S. (2012). A role for primary cilia in glutamatergic synaptic integration of adult-born neurons. Nat. Neurosci. *15*, 399–405, S391.

Laggerbauer, B., Ostareck, D., Keidel, E.M., Ostareck-Lederer, A., and Fischer, U. (2001). Evidence that fragile X mental retardation protein is a negative regulator of translation. Hum. Mol. Genet. *10*, 329–338.

Lee, B., Lee, K., Panda, S., Gonzales-Rojas, R., Chong, A., Bugay, V., Park, H.M., Brenner, R., Murthy, N., and Lee, H.Y. (2018). Nanoparticle delivery of CRISPR into the brain rescues a mouse model of fragile X syndrome from exaggerated repetitive behaviours. Nat. Biomed. Eng. *2*, 497–507.

Lee, H.Y., Ge, W.P., Huang, W., He, Y., Wang, G.X., Rowson-Baldwin, A., Smith, S.J., Jan, Y.N., and Jan, L.Y. (2011). Bidirectional regulation of dendritic voltage-gated potassium channels by the fragile X mental retardation protein. Neuron *72*, 630–642.

Lee, J.H., and Gleeson, J.G. (2010). The role of primary cilia in neuronal function. Neurobiol. Dis. *38*, 167–172.

Li, G., and Pleasure, S.J. (2005). Morphogenesis of the dentate gyrus: what we are learning from mouse mutants. Dev. Neurosci. *27*, 93–99.

Luo, Y., Shan, G., Guo, W., Smrt, R.D., Johnson, E.B., Li, X., Pfeiffer, R.L., Szulwach, K.E., Duan, R., Barkho, B.Z., et al. (2010). Fragile X mental retardation protein regulates proliferation and differentiation of adult neural stem/progenitor cells. PLoS Genet. *6*, e1000898.

Mathews, E.A., Morgenstern, N.A., Piatti, V.C., Zhao, C., Jessberger, S., Schinder, A.F., and Gage, F.H. (2010). A distinctive layering pattern of mouse dentate granule cells is generated by developmental and adult neurogenesis. J. Comp. Neurol. *518*, 4479–4490.

Mühlhans, J., Brandstätter, J.H., and Giessl, A. (2011). The centrosomal protein pericentrin identified at the basal body complex of the connecting cilium in mouse photoreceptors. PLoS One *6*, e26496.

Rhee, S., Kirschen, G.W., Gu, Y., and Ge, S. (2016). Depletion of primary cilia from mature dentate granule cells impairs hippocampus-dependent contextual memory. Sci. Rep. *6*, 34370.

Spencer, C.M., Alekseyenko, O., Hamilton, S.M., Thomas, A.M., Serysheva, E., Yuva-Paylor, L.A., and Paylor, R. (2011). Modifying behavioral phenotypes in Fmr1KO mice: genetic background differences reveal autistic-like responses. Autism Res. *4*, 40–56.

Tuz, K., Bachmann-Gagescu, R., O'Day, D.R., Hua, K., Isabella, C.R., Phelps, I.G., Stolarski, A.E., O'Roak, B.J., Dempsey, J.C., Lourenco, C., et al. (2014). Mutations in CSPP1 cause primary cilia abnormalities and Joubert syndrome with or without Jeune asphyxiating thoracic dystrophy. Am. J. Hum. Genet. *94*, 62–72.

Urbán, N., and Guillemot, F. (2014). Neurogenesis in the embryonic and adult brain: same regulators, different roles. Front. Cell Neurosci. *8*, 396.

Veland, I.R., Awan, A., Pedersen, L.B., Yoder, B.K., and Christensen, S.T. (2009). Primary cilia and signaling pathways in mammalian development, health and disease. Nephron Physiol. *111*, p39–53.

Yu, D.X., Marchetto, M.C., and Gage, F.H. (2014). How to make a hippocampal dentate gyrus granule neuron. Development *141*, 2366–2375.

Zorio, D.A., Jackson, C.M., Liu, Y., Rubel, E.W., and Wang, Y. (2017). Cellular distribution of the fragile X mental retardation protein in the mouse brain. J. Comp. Neurol. *525*, 818–849.

Stem Cell Reports, Volume *15*

Supplemental Information

Primary Ciliary Deficits in the Dentate Gyrus of Fragile X Syndrome

Bumwhee Lee, Shree Panda, and Hye Young Lee

Supplemental Experimental Procedures

Materials. Paraformaldehyde and D(+)-Sucrose were purchased from Acros Organics; Sodium Citrate Dihydrate, Phosphate Buffered Saline (PBS), and Superfrost Plus Microsope Slides from Fisher Scientific; Tissue-Plus O.C.T. Compound from Fisher Healthcare; Isoflurane from Vetone; ProLong Gold Antifade Reagent with DAPI from Molecular Probes; Embedding Molds from Thermo Scientific; Goat Serum from Gibco; PowerUp SYBR Green Master Mix from Applied Biosystems; and BrdU and SuperScript III First-Strand Synthesis kit from Invitrogen.

Antibodies. The following primary antibodies were used: rabbit anti-AC3 (1:500; Santa Cruz; SC588), rabbit anti-AC3 (1:2000; EnCor Biotechnology Inc.; RPCA-ACIII), rabbit anti-Arl13b (1:750; Proteintech; 17711-1-AP), rabbit anti-HOPX (1:500; Proteintech, 11419-1-AP), rat anti-BrdU (1:150; Novus; NB500-169), mouse anti-BLBP (1:300; Abcam; ab131137), mouse anti-FMRP (1:250; BioLegend; 843701), mouse anti-NeuN (1:500; Chemicon; MAB377), mouse anti-S100β (1:100; Santa Cruz; sc-393919), mouse anti-pericentrin (1:250, BD Biosciences; 611814), and chicken anti-calbindin (1:400; Encor Biotechnology Inc.; CPCA-Calb). For secondary antibodies: donkey anti-rat IgG-Alexa Fluor 488, (1:250), goat anti-rabbit-Cy3 (1:500), donkey anti-mouse Fcγ fragment-Cy5 (1:500), and donkey anti-chicken IgG-Alexa Fluor 647 (1:500) from Jackson ImmunoResearch Laboratories, Inc.

Vaginal Plug Formation. To monitor plug formation, fertile heterozygous female mice were housed with WT male mice. The following morning, females were checked for the presence of vaginal plugs. If a plug was present, the female was removed to a separate cage. If no plug was detected, the female remained in the cage with the male. Plug checks were performed every morning.

RNA Extraction from Mouse Brains and qRT-PCR. The DG was dissected from the hippocampus of postnatal mice in ice-cold PBS. After adding 800 µL of TRIzol, whole embryonic brains or the dissected DG were homogenized, treated with 160 µL of chloroform, and centrifuged for 15 min at 4°C. The aqueous phase of the sample was removed by pipetting and 400 µL of 100% isopropanol was added. After being centrifuged for 10 min, the supernatant was removed from the tube, and then the pellet was washed with 75% ethanol and centrifuged for 5 min. Afterwards, the supernatant was removed and the pellet was dissolved in DNase- and RNase-free water. 1 µg of RNA was reverse-transcribed using the SuperScript III First-Strand Synthesis kit (Invitrogen). qRT-PCR analysis was performed using PowerUp SYBR Green Master Mix (Applied Biosystems) with the primers listed in Table 1. The relative expression from RNA samples was analyzed using the $2^{-\Delta\Delta CT}$ method. Values of *Gli1* mRNA were normalized by the peptidylprolyl isomerase A (*Ppia*) housekeeping gene expression levels.

Table 1. qRT-PCR primers.

Gli1 (Gli1) F	CACTACCTGGCCTCACACCT
Gli1 (Gli1) R	GTACTCGGTTCGGCTTCTCC
Ppia (PPIA) F	GAGCTGTTTGCAGACAAAGTTC
Ppia (PPIA) R	CCCTGGCACATGAATCCTGG

Immunostaining. For immunostaining, all sections were post-fixed by methanol for 10 min at -20°C, followed by antigen retrieval for 15 min. After being washed twice with PBS for 5 min, the sections were incubated overnight with blocking solution (5% goat serum, 0.01% Triton-X 100 in PBS). The following day, the sections were incubated with the appropriate primary antibodies for 4 h at room temperature and then washed 3 times with PBS for 7 min, followed by incubation with secondary antibodies for 2 h at room temperature afterwards. After additionally being washed 3 times with PBS for 7 min and with 70% ethanol for 1 min, the sections were mounted with ProLong Gold Antifade Reagent with DAPI. Immunostained sections were kept in 4°C. For BrdU immunostaining, the brain tissues were additionally pretreated in 2 M HCl for 15-30 min at 37°C as previously reported (Amador-Arjona et al., 2011).

Imaging and Analysis. Images were taken randomly in each brain region of interest by Zeiss LSM710 Confocal microscopy with a 40x oil objective lens and 2.0 zoom at a 10 μm range with 1 μm intervals and a total of 11 slices. To analyze primary cilia or basal bodies of primary cilia, the number of $AC3^+$, $Arl13b^+$ (for primary cilia), or $pericentrin^+$ cells (for basal bodies) were counted and normalized as indicated in the figure legends. To analyze the number of neurons, the number of $NeuN^+$ cells was counted and normalized by the number of $DAPI^+$ cells. Cells were counted by Image J software (NIH). To determine the relative FMRP expression levels in the DNe or the DG during embryonic development, images were taken by Zeiss Apotome fluorescence microscopy with a 10x lens. The fluorescence intensity of FMRP in a defined ROI where HOPX expresses in the DNe or the DG was analyzed using the Image J software (NIH). Mean fluorescence intensities were taken and background fluorescence signals (same region in *Fmr1* KO brain) were subtracted.

Data Availability. All data that support the findings of this study are available from the corresponding author upon reasonable request.

Supplemental References

Amador-Arjona, A., Elliott, J., Miller, A., Ginbey, A., Pazour, G.J., Enikolopov, G., Roberts, A.J., and Terskikh, A.V. (2011). Primary cilia regulate proliferation of amplifying progenitors in adult hippocampus: implications for learning and memory. J Neurosci *31*, 9933-9944.

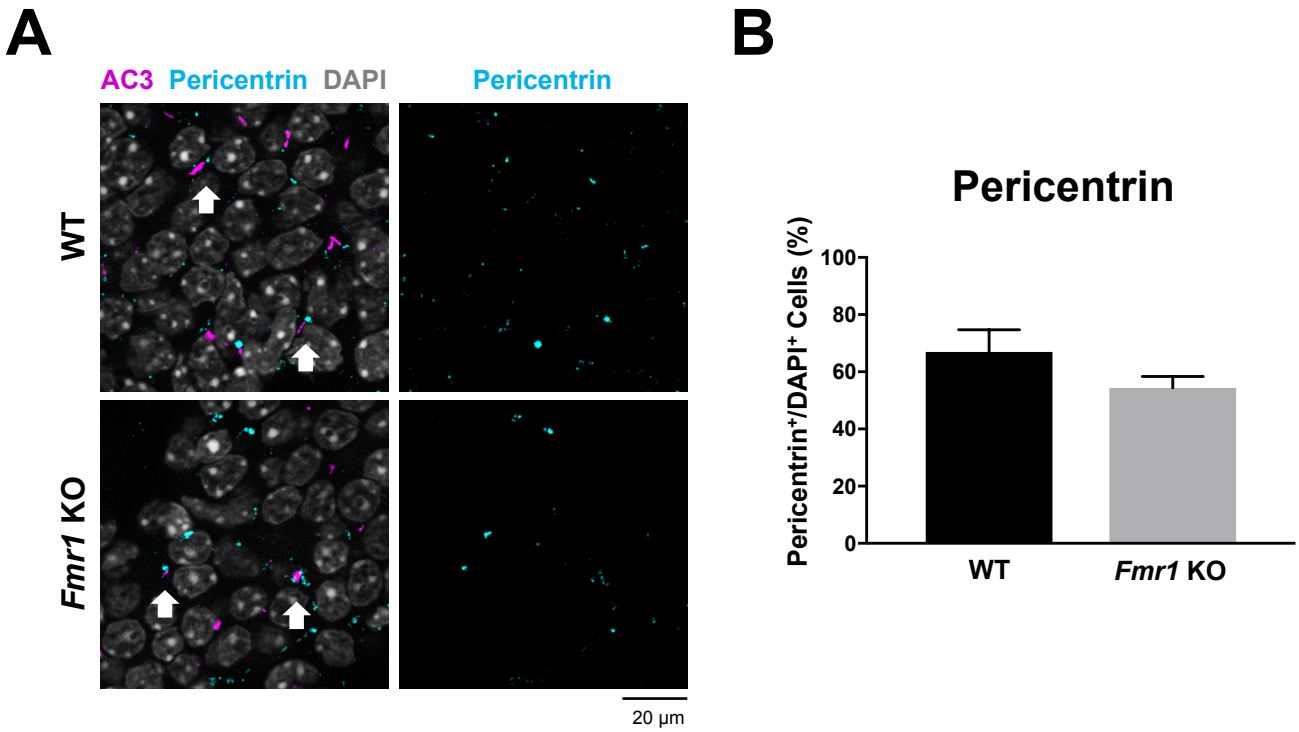

Figure S1. No significant reduction in the number of basal bodies is found in the DG of *Fmr1* KO mice. Related to Figure 1. (A) Immunostaining of AC3 (magenta) and pericentrin (cyan) with DAPI nuclear staining (gray) in the DG of P60 WT or *Fmr1* KO mice. White arrows, $AC3^{+}$;$pericentrin^{+}$ cells. (B) Quantification of the percentage of $pericentrin^{+}$ cells among $DAPI^{+}$ cells. n = 16, mean ± SEM. Student's unpaired t test.

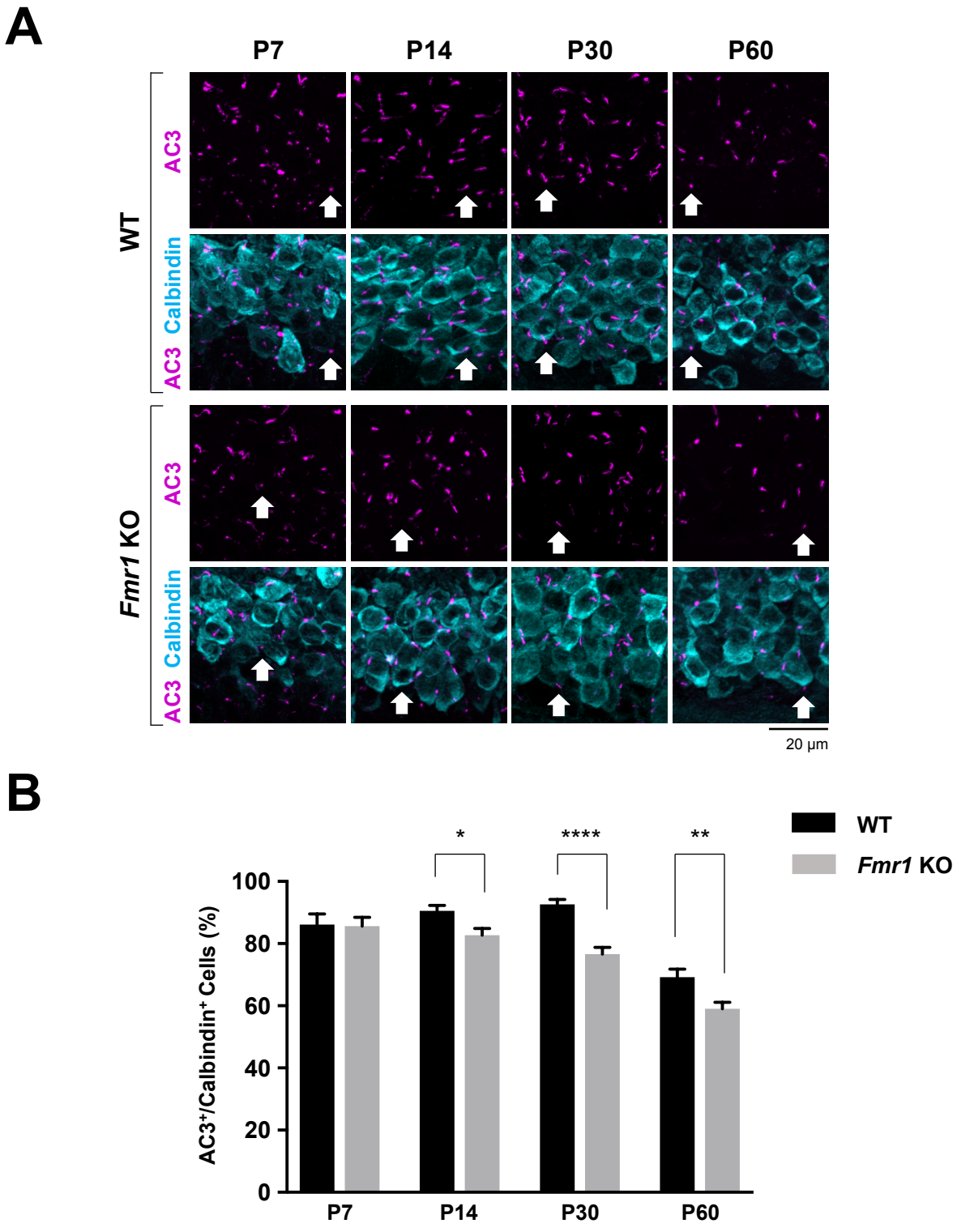

Figure S2. The number of primary cilia is reduced in calbindin$^+$ mature granule neurons in the DG of *Fmr1* KO mice. Related to Figure 4. (A) Immunostaining of AC3 (magenta) and calbindin (cyan) in the DG of P7, P14, P30, and P60 WT or *Fmr1* KO mice. White arrows, AC3$^+$;calbindin$^+$ cells. (B) Quantification of the percentage of AC3$^+$ cells among calbindin$^+$ cells. n = 8, mean ± SEM. Student's unpaired t test. *p < 0.05, **p < 0.01, ****p < 0.0001.

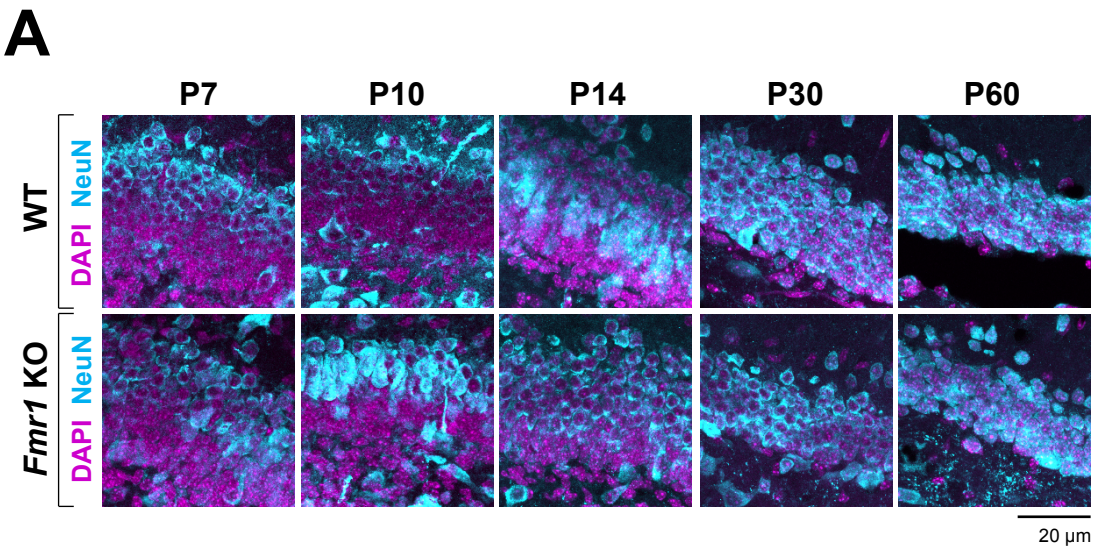

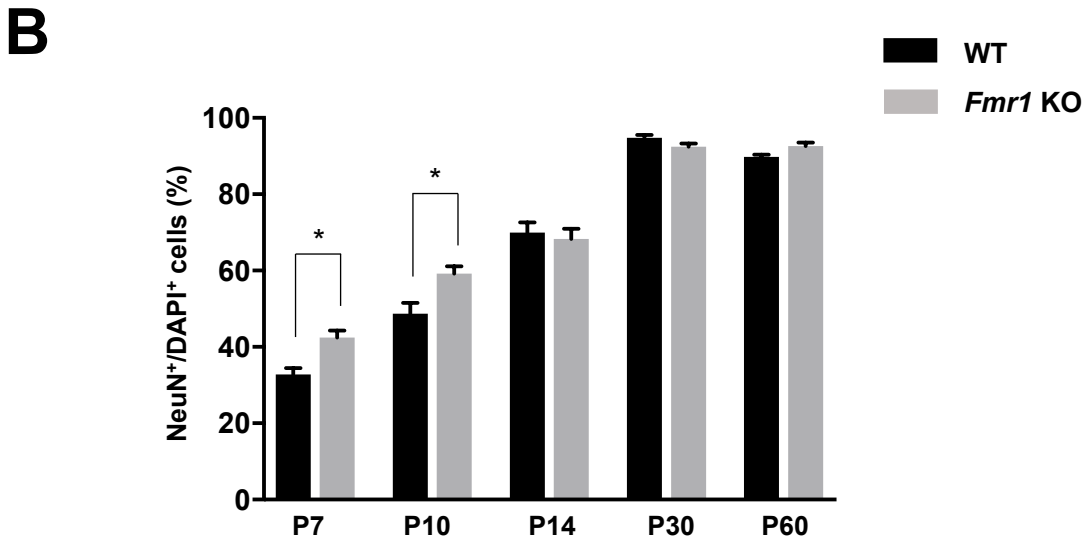

Figure S3. The number of NeuN⁺ mature granule neurons are not reduced during the DG development of postnatal *Fmr1* KO mice. Related to Figure 4. (A) Immunostaining of NeuN (cyan) with DAPI nuclear staining (magenta) in the DG of P7, P10, P14, P30, and P60 WT (top) or *Fmr1* KO (bottom) mice. (B) Quantification of the percentage of NeuN⁺ cells among DAPI⁺ cells. n = 8, mean ± SEM. Student's unpaired t test. *p < 0.05.

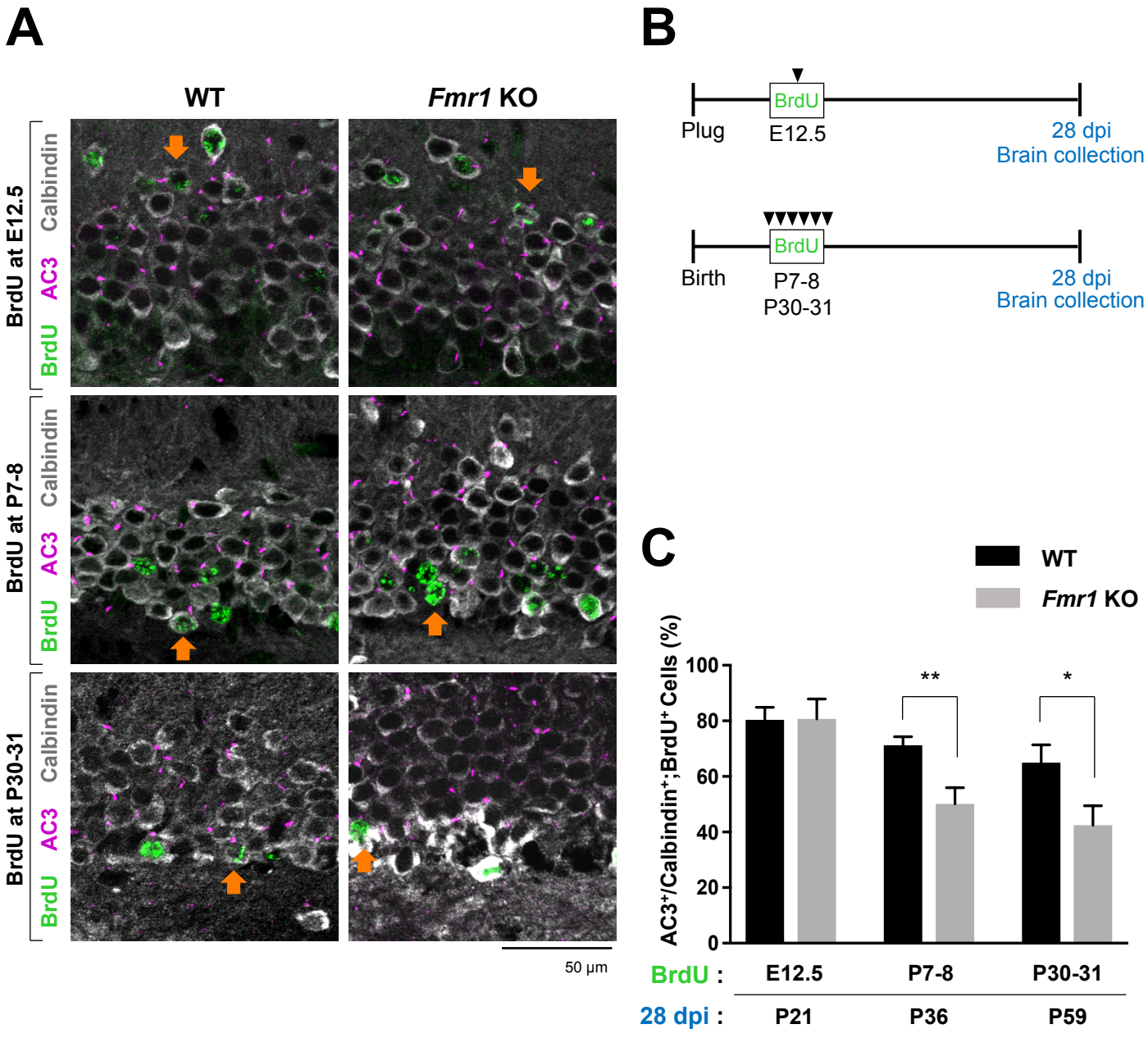

Figure S4. Newborn neurons (calbindin$^+$;BrdU$^+$) originated from the SGZ exhibit primary cilia loss in the DG of *Fmr1* KO mice. Related to Figure 6. BrdU was administrated by intraperitoneal injection into WT or *Fmr1* KO mice at E12.5, P7-8, or P30-31 followed by brain collection at 28 days post injection (dpi). (A) Immunostaining of AC3 (magenta), calbindin (gray), and BrdU (green) in the DG of BrdU-treated WT or *Fmr1* KO mice. Orange arrows, AC3$^+$;calbindin$^+$;BrdU$^+$ cells. Inner layer (toward hilus) of the DG is located on the lower side of images. (B) Schematic view of BrdU treatment and collection of WT or *Fmr1* KO mice. (C) Quantification of the percentage of AC3$^+$ cells among calbindin$^+$;BrdU$^+$ newborn neurons originating at E12.5, P7-8, or P30-31 in WT and *Fmr1* KO mice (28 dpi: P21, P36, or P59). n = 8, mean ± SEM, Student's unpaired t test. *p < 0.05, **p < 0.01.

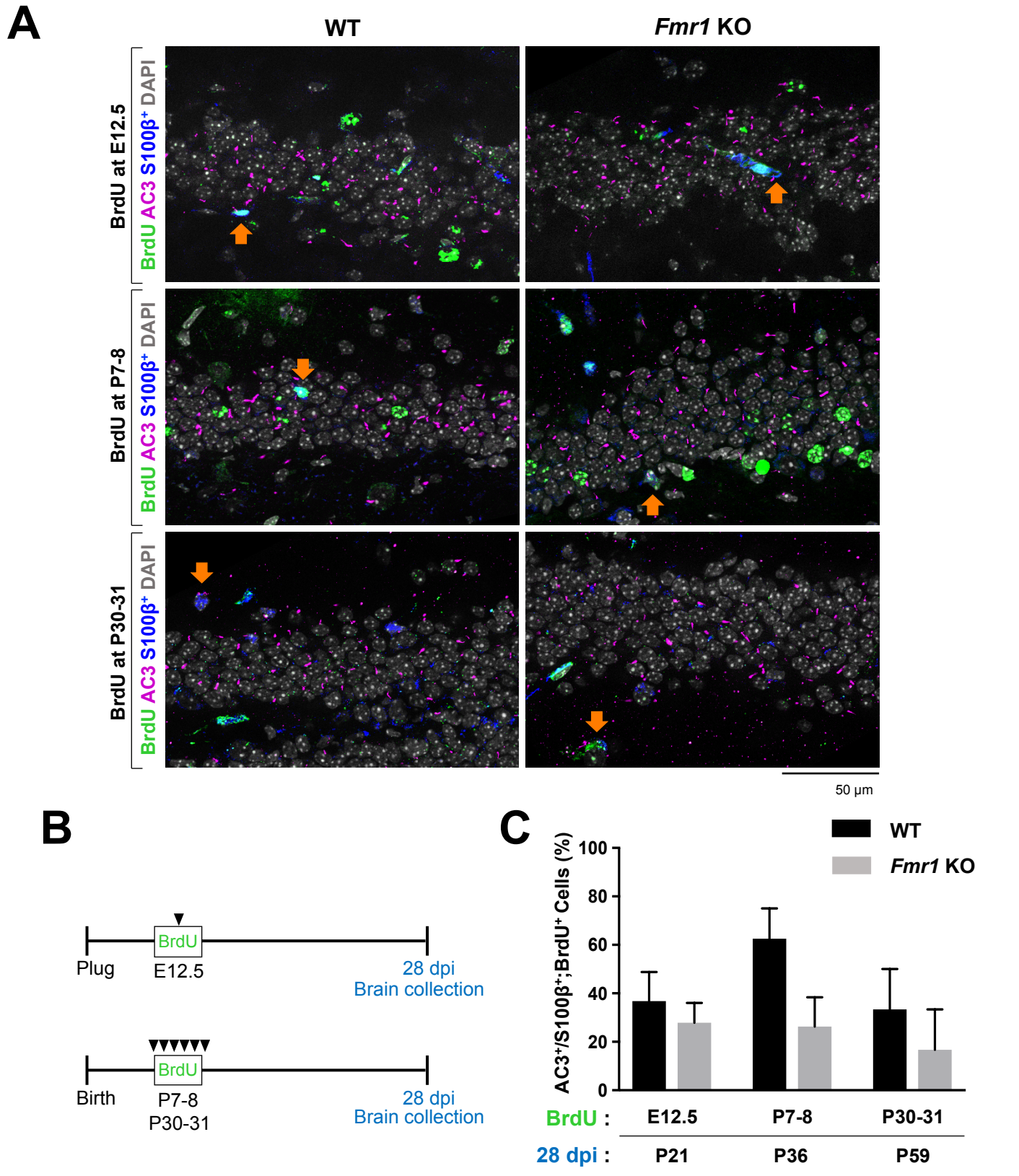

Figure S5. Newly differentiated astrocytes (S100β⁺;BrdU⁺) do not exhibit primary cilia loss in the DG of *Fmr1* KO mice. Related to Figure 6. BrdU was administrated by intraperitoneal injection into WT or *Fmr1* KO mice at E12.5, P7-8, or P30-31 followed by brain collection at 28 days post injection (dpi). (A) Immunostaining of AC3 (magenta), S100β (blue), and BrdU (green) with DAPI nuclear staining (gray) in the DG of BrdU-treated WT or *Fmr1* KO mice. Orange arrows, AC3⁺;S100β⁺;BrdU⁺ cells. Inner layer (toward hilus) of the DG is located on the lower side of images. (B) Schematic view of BrdU treatment and collection of WT or *Fmr1* KO mice. (C) Quantification of the percentage of AC3⁺ cells among S100β⁺;BrdU⁺ newly differentiated astrocytes originating at E12.5, P7-8, or P30-31 in WT and *Fmr1* KO mice (28 dpi: P21, P36, or P59). n = 8, mean ± SEM, Student's unpaired t test.

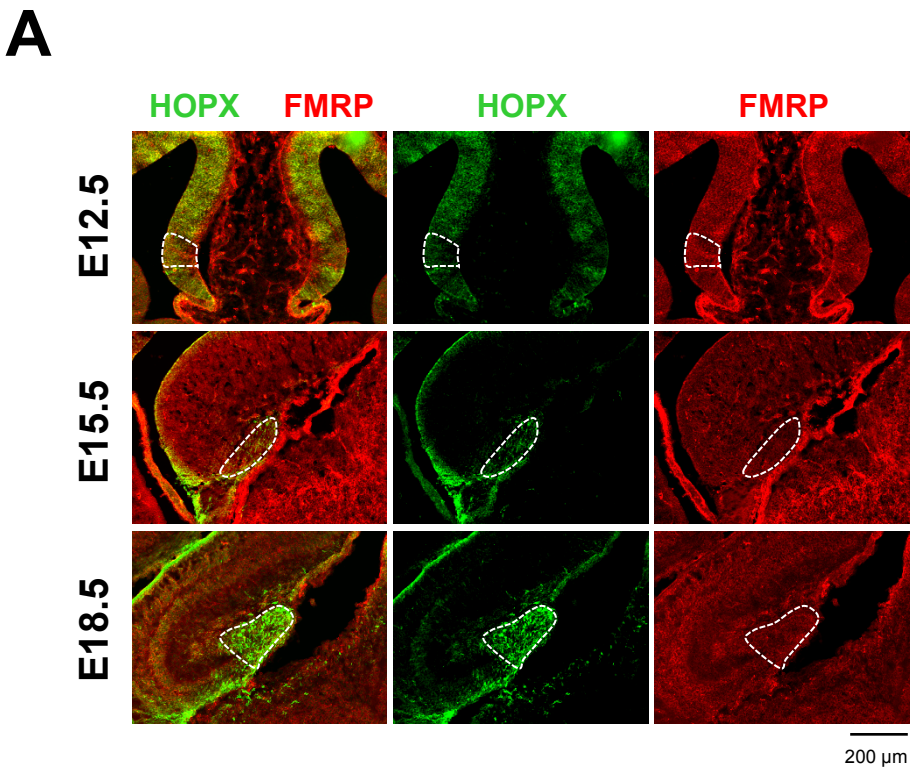

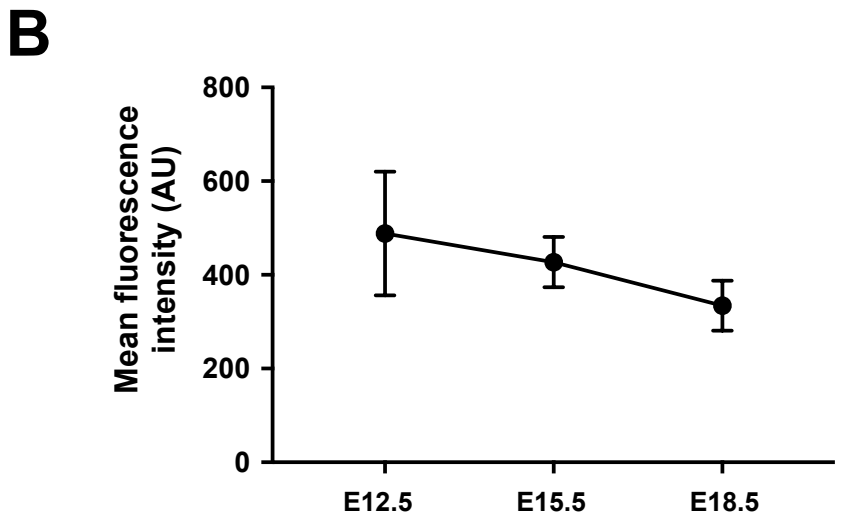

Figure S6. FMRP expression levels are not significantly changed during embryonic development between E12.5 and E18.5. Related to Figure 6. (A) Immunostaining of HOPX (green) and FMRP (red) in the DNe or DG of E12.5, E15.5, and E18.5 WT embryos. FMRP expression levels were analyzed in the DNe or DG (white dashed line) where HOPX expresses. (B) Mean intensity of FMRP was analyzed in E12.5, E15.5, and E18.5 from the DNe or DG of WT embryos and was subtracted by the mean intensity of FMRP in *Fmr1* KO mice. n = 4. mean ± SEM. One-way ANOVA.